The voltage-gated Na$^+$ channel Na$_V$BP has a role in motility, chemotaxis, and pH homeostasis of an alkaliphilic *Bacillus*

Masahiro Ito*†, Haoxing Xu†‡, Arthur A. Guffanti§, Yi Wei§, Lior Zvi§, David E. Clapham‡, and Terry A. Krulwich§¶

*Faculty of Life Sciences, Toyo University, Oura-gun, Gunma 374-0193, Japan; ‡Howard Hughes Medical Institute, Department of Cardiovascular Research, Children's Hospital and Department of Neurobiology, Harvard Medical School, Boston, MA 02115; and §Department of Pharmacology and Biological Chemistry, Mount Sinai School of Medicine, New York, NY 10029

The prokaryotic voltage-gated Na$^+$ channel, NaChBac, is one of a growing channel superfamily of unknown function. Here we show that Na$_V$BP, the NaChBac homologue encoded by *ncbA* in alkaliphilic *Bacillus pseudofirmus* OF4, is a voltage-gated Na$^+$ channel potentiated by alkaline pH. Na$_V$BP has roles in motility, chemotaxis, and pH homeostasis at high pH. Reduced motility of bacteria lacking functional Na$_V$BP was reversed by restoration of the native channel but not by a mutant Na$_V$BP engineered to be Ca^{2+}-selective. Motile *ncbA* mutant cells and wild-type cells treated with a channel inhibitor exhibited behavior opposite to the wild type in response to chemoeffectors. Mutants lacking functional Na$_V$BP were also defective in pH homeostasis in response to a sudden alkaline shift in external pH under conditions under which cytoplasmic [Na$^+$] is limiting for this crucial process. The defect was exacerbated by mutation of *motPS*, the motility channel genes. We hypothesize that activation of Na$_V$BP at high pH supports diverse physiological processes by a combination of direct and indirect effects on the Na$^+$ cycle and the chemotaxis system.

The founding member of the recently discovered Na$_V$Bac superfamily of bacterial voltage-gated Na$^+$ channels is the NaChBac channel of alkaliphilic *Bacillus halodurans* C-125 (1–3). NaChBac is a channel protein containing six transmembrane domains that strongly resembles one of the repeats of mammalian Na$_V$ or voltage-gated calcium channel channels (1). The alkaliphile Na$_V$Bac is highly Na$^+$-selective when expressed in mammalian cells, although its activation and inactivation kinetics are slow relative to mammalian Na$_V$s (1). Including Na$_V$BP, the NaChBac homologue from alkaliphilic *Bacillus pseudofirmus* OF4 studied here, 13 Na$_V$Bac superfamily members have been identified in diverse bacteria whose common themes include marine and/or alkaline niches (3) (Fig. 1*A*). High-resolution structural studies of other bacterial ion channels have had a tremendous impact on the field of channel biophysics (3, 5). By contrast, the physiological roles of bacterial channels have often remained unresolved, although clarification of their roles would significantly impact the realm of microbial physiology (5).

Physiological roles are expected for Na$_V$BP in motility and/or pH homeostasis at elevated pH, because these processes depend on Na$^+$ in alkaliphilic, alkaline-tolerant, and marine bacteria (6–9). Na$^+$/H$^+$ antiporters catalyze H$^+$ accumulation coupled to Na$^+$ efflux, thereby maintaining a cytoplasmic pH well below the high external pH (pH$_o$) in alkaliphilic *Bacillus* species (Fig. 1*B*). In complete growth medium, Na$^+$-coupled solute uptake systems are a major contributor of the cytoplasmic Na$^+$ required for antiporter function (8, 10, 11). A Na$^+$ channel that opened at high pH$_o$ was predicted to provide an important alternative Na$^+$ reentry route for support of cytoplasmic pH homeostasis when Na$^+$ and solutes that enter with Na$^+$ are scarce (7). The Na$^+$-translocating Mot channel that energizes flagellar rotation was a prime candidate for such a channel, because alkaliphile motility is restricted to alkaline pH values (9, 12). However, no

pH homeostasis defect was found upon disruption of the genes encoding MotPS, the Na$^+$-translocating channel proteins required for motility of alkaliphilic *B. pseudofirmus* OF4 (13). A role for Na$_V$BP in pH homeostasis was thus an attractive possibility. Here we measure the ion channel function of Na$_V$BP and its physiological role in *B. pseudofirmus* OF4.

Materials and Methods

Bacterial Strains, Plasmids, and Growth Conditions. The bacterial strains and plasmids used in this study are listed in Table 4, which is published as supporting information on the PNAS web site. Strains of alkaliphilic *B. pseudofirmus* OF4 were grown at 30°C either in semidefined malate-yeast extract (MYE) medium (12) at pH 7.5 or 10.5. Ca^{2+} (0.65 mM) was added to MYE for experiments testing mutant complementation by the Ca^{2+}-specific variant of the channel.

Sequencing of *B. pseudofirmus* OF4 Na$_V$BP-Encoding Gene ncbA. PCR was carried out by using a primer set designed from a conserved region of the NaChBac-encoding genes of *Bacillus halodurans* C-125 and *Magnetococcus* sp. MC-1. Genomic DNA from *B. pseudofirmus* OF4 was the template. The initial PCR product was used for characterization of a larger region using a series of inverse PCR reactions. The method and primers are detailed in Table 5, which is published as supporting information on the PNAS web site. The sequence of 2,542 bp of a region containing the apparently monocistronic *ncbA* gene was deposited in Gen-Bank.

Mammalian Electrophysiology. *ncbA* was cloned into the mammalian expression vector pTracer-CMV3 (Invitrogen), yielding pCMV-SC7 (see *Supporting Text*, which is published as supporting information on the PNAS web site). The plasmid pCMV-SC-Ca was similarly prepared and encodes a triple mutant of *ncbA*: $_{191}$L*ESW*AS$_{196}$→ $_{191}$L*DDW*AD$_{196}$. Mutations were introduced into the Na$_V$BP DNA by site-directed mutagenesis (QuickChange site directed mutagenesis kit; Stratagene). CHO-K1 cells were grown in DMDM (Invitrogen) supplemented with 10% FBS at 37°C under 5% CO$_2$. DNA was transfected by using Lipofectamine 2000 (Invitrogen), plated
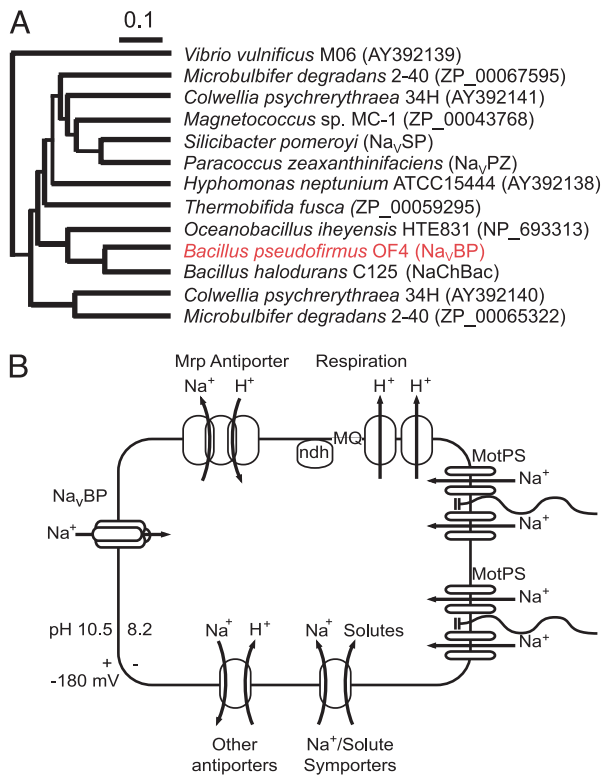
Fig. 1. The place of Na_VBP in the Na_VBac superfamily and its potential participation in the Na^+ cycle of alkaliphilic *B. pseudofirmus* OF4. (*A*) Phylogenic tree of bacterial NaChBac homologues. A multiple alignment was calculated by using the CLUSTALW program (http://clustalw.genome.jp). The tree was then generated by using the neighbor-joining method (Njplot) (4). Branch lengths are proportional to the sequence divergence and can be measured relative to the bar shown (Bar = 0.1 substitution per amino acid site). The GenBank accession numbers are indicated in parentheses. (*B*) Schematic diagram of the Na^+ cycle of alkaliphilic *B. pseudofirmus* OF4. Na^+/H^+ antiporters, particularly the Mrp antiporter depicted here (10), catalyze net proton accumulation in the cytoplasm in cells that are extruding protons during respiration. Na^+ reentry in support of pH homeostasis is achieved by Na^+:solute symporters (8). When Na^+ entry is limiting, e.g., at low $[Na^+]$ or a paucity of symporter substrates, pH-activated Na^+ channels are hypothesized to provide an important Na^+ reentry path (7–9). Candidates for such channels are the Na_VBP channel (1–3) and the MotPS channel (8).

onto coverslips, and recordings were made after 24 h. Unless otherwise stated, the pipette solution contained 147 mM Cs^+, 120 mM methane-sulfonate, 8 mM NaCl, 10 mM EGTA, 2 mM Mg-ATP, and 20 mM Hepes (pH 7.4). The bath solution contained 140 mM NaCl, 10 mM $CaCl_2$, 5 mM KCl, 20 mM Hepes (pH 7.4), and 10 mM glucose. For high pH solutions, NaCl was replaced with equimolar NaOH (final pH adjusted using NaOH and Trizma base). Experiments were conducted at $22°C \pm 2°C$. Unless otherwise indicated, all chemicals were dissolved in water. Nifedipine (dissolved in DMSO) was purchased from Sigma.

Disruption of the *ncbA* Gene in *B. pseudofirmus* OF4 and Restoration of the Gene. The *ncbA* gene was replaced almost entirely by a Sp^R cassette to produce strain SC34. This gene replacement and restoration of a functional *ncbA* gene to SC34 and its derivative SC34-M were achieved by using an approach described earlier (14). A silent mutation was introduced to serve as a marker as well as to facilitate the construction. Protoplast transformation (14) was used to transform alkaliphile strains with low copy control vector, pYM1 (Table 4), and recombinant pYM1 ex-

pressing *ncbA*, pSC, or the mutant version, pSC-Ca, from the native *ncbA* promoter.

Motility and Chemotaxis Assays. Motility was assessed from the diameter of alkaliphile colonies on soft agar plates of MYE, pH 10.5, solidified with 0.3% agar; in this assay, nonmotile strains produce large, dense colonies that do not extend significantly beyond the initial inoculation site (13). Chemotaxis was assayed by a modification of the capillary assay method of Adler (15). Cells of up-motile wild-type (wild-type-M) and *ncbA* mutant (SC34-M) were grown on MYE, pH 10.5, washed and resuspended in 100 mM Na_2CO_3–$NaHCO_3$ buffer containing 1 mM potassium phosphate and 0.1 mM $MgSO_4$. The pH was adjusted to 8.5, and the turbidity was adjusted to a final A_{600} of 0.4. A covered well on a glass slide was filled with 250 μl of cell suspension. The open end of a capillary tube, filled with the control buffer or test buffer and sealed at the other end, was inserted into the well. After 1 hour at 30°C, the capillary tube was rinsed, broken open, and the contents were expelled into 1 ml of pH 10.5 dilution buffer (15). Colony counts were conducted on solidified MYE, pH 10.5.

pH Homeostasis Assays and Transmembrane Electrical Potential (Potential ($\Delta\Psi$) Measurements. Cells growing logarithmically on MYE, pH 10.5, were harvested, washed, and resuspended to ≈ 1 mg of cell protein/ml in bicarbonate-carbonate buffer, pH 8.5, containing the indicated concentrations of Na^+. After equilibration for 10 min at 20°C, the cells were diluted 1:25 into buffers with the different $[Na^+]$ that were adjusted so that the final pH was 10.5. The cytoplasmic pH and the $\Delta\Psi$ were determined, respectively, from the distribution of radiolabeled methylamine and tetraphenylphosphonium bromide as described (14, 16).

Results

***ncbA* Encodes Na_VBP, a Six-Transmembrane Domain (6TM) Protein Belonging to the Na_VBac Superfamily of Bacterial Voltage-Gated Na^+-Selective Ion Channels.** Hydrophobicity analysis of Na_VBP predicted a 6TM architecture, a general Na_VBac feature, and significant sequence homology to NaChBac (69% identity; 81% homology); it seemed likely that Na_VBP also functions as a voltage-gated Na^+ channel. Voltage-dependent Na^+ channels are triggered by depolarization of the transmembrane voltage, rapidly increasing the amount of Na^+ ions they pass into the cell above a set voltage range, and more slowly inactivating over time. Transfected CHO-K1 cells expressing Na_VBP exhibited large (up to 10 nA) voltage-activated inward currents (Fig. 2*A*) not observed in nontransfected or mock-transfected cells (data not shown). Na_VBP-mediated current (I_{NavBP}) reversed at $\approx +70$ mV (Fig. 2*B*), close to the Nernst equilibrium potential for Na^+ (+72 mV) under our recording conditions. Extracellular cation replacement resulted in complete (*N*-methyl-D-glucammonium, $NMDG^+$) or nearly complete (105 mM Ca^{2+}) removal of voltage-dependent I_{NavBP} inward current (not shown). Thus Na_VBP forms a voltage-gated Na^+-selective ion channel similar to currents mediated by other Na_VBac channels (1, 3). Characteristically for Na_VBac currents, I_{NavBP} activated and inactivated much more slowly than mammalian Na_V channels (Fig. 2*A*). In cells transfected by a pore mutant designed to convert the Na^+-selective Na_VBP channel into a Ca^{2+}-selective channel, we observed a voltage-gated Ca^{2+}-selective conductance as reported for CaChBac (data not shown) (2).

We found that I_{NavBP} was dramatically potentiated when we increased the bath pH from 7.4 to 9 (Fig. 2 *A* and *B*). At pH 9.0, both the activation and peak voltage were shifted ≈ -30 mV (hyperpolarized; Fig. 2*B*) relative to pH 7.4. Due to the slow recovery from inactivation for Na_VBac channels and the difficulty of maintaining patch integrity at very high pH, we applied repeated continuous incremental increases in transmembrane
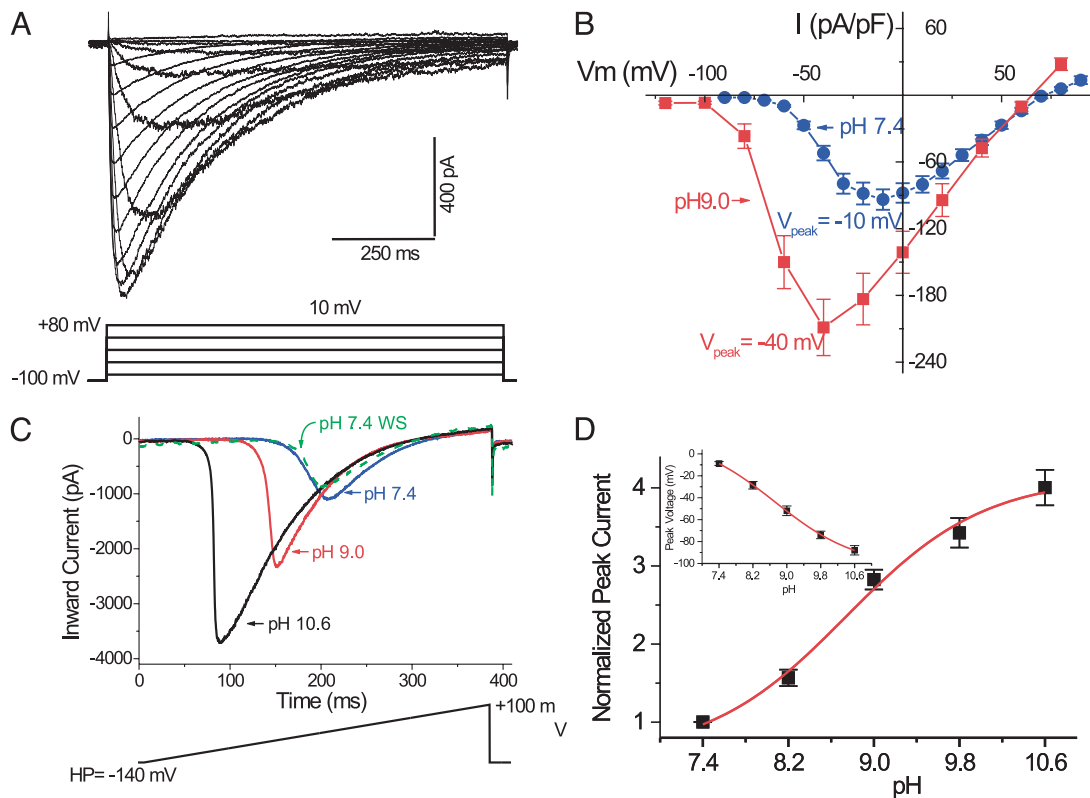
Fig. 2. Na$_V$BP is a voltage-gated Na$^+$ channel modulated by extracellular alkaline pH. (*A*) Representative traces (*Upper*) of I_{NavBP} activated by the voltage protocol shown. Holding potential ($V_{HP} = -100$ mV). The cell was bathed in 10 mM Ca^{2+} external solution (140 mM Na$^+$/10 mM Ca^{2+}/5 mM K$^+$ pipette; 147 mM Cs$^+$/8 mM Na$^+$; see *Materials and Methods*). (*B*) Averaged peak current–voltage (*I–V*) relation of Na$_V$BP in standard bath solution at pH 7.4 (blue, $n = 19$, $V_{HP} = -100$ mV), and pH 9.0 (red, $n = 11$, $V_{HP} = -130$ mV), normalized by cell capacitance (pF). (*C*) Increasing pH$_o$ reversibly potentiated I_{NavBP} generated by a ramp protocol (-140 mV to $+100$ mV in 380 ms, $V_{HP} = -140$ mV). (*D*) pH$_o$-dependent changes on the normalized amplitude of the peak inward current ($n = 9$; $\pm$ SEM). The pH$_o$-dependent shifts of the peak voltage is plotted (*Inset*).

voltage (ramp protocol) to study the effects of pH on I_{NavBP}. A similar approach has been used to define the neuronal persistent Na$^+$ current (17). When the bath pH was raised, I_{NavBP} in response to the voltage ramp was dramatically increased (Fig. 2*C*). This potentiation was dose-dependent (Fig. 2*D*) and reversible (Fig. 2*C*). Changing pH from 7.4 to 10.6 increased the amplitude of the peak current ≈4-fold (Fig. 2*D*) and shifted the voltage at which current was at its maximum from −10mV to −90mV (Fig. 2*D Inset*).

To more accurately probe the mechanism of pH-dependent potentiation, we evaluated the steady-state and voltage-dependent activation of I_{NavBP} (Fig. 3). Steady-state inactivation of the channel was determined by sequential depolarizations to test voltages followed by voltage clamp to the peak of activation at −10 mV (Fig. 3*A*). A Boltzmann fit of the averaged steady-state inactivation curve yielded 50% inactivation at −57 ± 0.3 mV ($n = 14$) and slope factor (κ) of 6.7 ± 0.3 mV/*e*-fold change of channel activity (Fig. 3 *A* and *C*). At pH 9.0, however, 50%
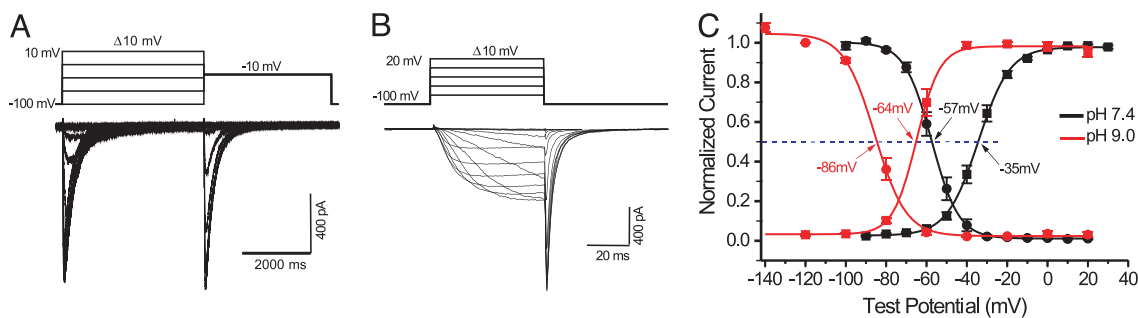

Fig. 3. Alkaline pH shifts the voltage dependence of Na$_V$BP activation and state-steady inactivation of I_{NavBP} to more hyperpolarized potentials. (*A*) I_{NavBP} steady-state inactivation currents (pH 7.4). After a 4-s prepulse, the currents inactivated to a steady-state level and were reactivated by a second 4-s depolarizing pulse (−10 mV). $V_{HP} = -100$ mV. The intersweep interval was 20 s. (*B*) I_{NavBP} deactivation tail currents. After prepulses of varying depolarization (from −90 to +20 mV, increments = +10 mV), tail currents were measured upon return to the holding potential (V_{HP}, −100 mV). The intersweep interval was 20 s. (*C*) Normalized activation curve and steady-state inactivation curve at pH 7.4 (black) and pH 9.0 (red). At pH 7.4 ($V_{HP} = -100$ mV), the half activation ($V_{1/2}$) is −35 ± 0.3mV ($n = 16$, ± SEM) with a slope factor (κ) of 7.8 ± 0.3 mV per *e*-fold change in current. At pH 9.0 ($V_{HP} = -140$ mV), activation $V_{1/2}$ is −64 ± 0.7 mV ($n = 21$), and κ is 5.8 ± 0.6 mV/*e*-fold. The 50% steady-state inactivation is −57 ± 0.3 mV ($n = 14$) and −86 ± 0.9 mV ($n = 30$) at pH 7.4 and 9.0, respectively. κ is 6.7 ± 0.3 and 7.7 ± 0.7 mV/*e*-fold for pH 7.4 and 9.0, respectively .

Ito *et al*.

Table 1. Effect of Na$_V$BP status on *B. pseudofirmus* OF4 motility

Strain	Colony diameter, mm*	Tumbling[†]
Wild type	19.8 ± 1.2[‡]	±
SC34 (Δ*ncbA*)	9.1 ± 1.0	++
SC34-R (Δ*ncbA*, *ncbA* restored)	16.2 ± 0.8	+
Wild-type-M	37.5 ± 1.4	±
SC34-up motile	44.5 ± 3.9	++
SC34-up motile-R (*ncbA* restored)	46.2 ± 1.5	+
Wild-type/pYM1	19.1 ± 1.8	+
Wild-type/pSC	28.2 ± 2.2	++
Wild-type/pSC-Ca	18.5 ± 1.1	±
SC34/pYM1	11.4 ± 2.2	++
SC34/pSC	29.5 ± 4.0	+++
SC34/pSC-Ca	8.5 ± 0.5	++

*Measured after 18 hr on MYE medium, pH 10.5, solidified with 0.3% agar.
[†]Qualitative assessment by phase microscopic observations
[‡]Mean values of two to four independent experiments with standard deviations of the mean.

Table 2. Inverse chemotaxis behavior of *ncbA* mutant and Nifedipine-treated wild-type

Strain	Effector in capillary*	Positive chemotaxis[†]	Negative chemotaxis[†]
Wild-type-M	Aspartate	43.5 ± 2.8	—
SC34-M (Δ*ncbA*)	Aspartate	—	26.2 ± 3.7
SC34-MR (Δ*ncbA*, *ncbA* restored)	Aspartate	2.5 ± 0.4	—
Wild-type-M	Proline	83.0 ± 5.2	—
SC34-M	Proline	—	21.1 ± 4.1
Wild-type-M	Glucose	131.4 ± 4.3	—
SC34-M	Glucose	—	9.2 ± 1.1
Wild-type-M	pH 10.5	—	10.9 ± 0.6
SC34-M	pH 10.5	38.3 ± 3.5	—
Wild-type-M	pH 10.5 + 1 mM malate[‡]	27.3 ± 1.4	—
SC34-M	pH 10.5 + 1 mM malate[‡]	—	31.5 ± 3.6
Wild-type-M + 50 μM Nifedipine[§]	Aspartate	—	8.9 ± 1.3

*Chemoeffectors were added at 1 mM and, except where noted, the buffer pH inside the capillary was 8.5. The buffer pH outside the capillary was always pH 8.5.
[†]Positive chemotaxis is the number of cells (×10⁴) in the capillary tube with effector in excess of the cells found in the capillary tube without effector in the control experiment (pH 8.5 → pH 8.5, no effector present), whereas negative chemotaxis is the excess of cells (×10⁴) found in the capillary tube in the control without effector compared to the capillary tube with effector.
[‡]An additional control was conducted with 1 mM malate in the capillary at pH 8.5; the accumulation was indistinguishable from the standard control with pH 8.5 in both compartments and no effector.
[§]The control used for background correction was conducted in the presence of 50 μM Nifedipine.

inactivation occurred at a much more hyperpolarized potentials (-86 ± 0.9 mV, $n = 30$) with a slight increase in slope value (7.7 ± 0.7 mV/*e*-fold). Voltage-dependent activation was evaluated by measuring the deactivation tail currents (Fig. 3*B*). Activation was a steep function of voltage with $V_{1/2}$ of -35 ± 0.3 mV ($n = 16$) and slope factor (κ) of 7.8 ± 0.3 mV per *e*-fold change (Fig. 3*C*). At pH 9.0, $V_{1/2}$ was -64 ± 0.7 mV ($n = 21$) and κ was 5.8 ± 0.6 mV/*e*-fold. These changes in voltage sensitivity show that the channel is poised to initiate rapid entry of Na$^+$ and membrane depolarization at more negative potentials when pH$_o$ is high. Because bacterial resting transmembrane voltages are very negative (e.g., -150 mV) compared to eukaryotic cells (e.g., -70 mV), these bacteria are more likely to reach activation voltages at high pH. Similar to $I_{NaChBac}$, I_{NavBP} was sensitive to high concentrations of Nifedipine (30 μM, not shown).

The *B. pseudofirmus* OF4 *ncbA* Mutant Is Still Alkaliphilic but Exhibits a Motility Defect and Inverse Chemotaxis. Wild-type *B. pseudofirmus* OF4, the channel mutant SC34, and the SC34-R strain to which *ncbA* was restored all exhibited doubling times that ranged from 95 to 110 min at pH 7.5 and 70–75 min at pH 10.5. The growth yield of SC34 was reduced ≤20% relative to wild type on MYE, pH 10.5. Motility of wild-type *B. pseudofirmus* OF4 is restricted to pH ≥8 and is modest before selection of an up-motile variant (13). SC34 was even less motile than wild-type in liquid MYE, pH 10.5, with only ≈1% of the cells observed swimming relative to ≈20% of the wild type. The percentage of swimming SC34 cells increased slightly after longer incubation. In a motility assay on soft agar MYE plates at pH 10.5, the motility of the wild-type strain was twice that of SC34 after 18 h (Table 1). The diameter of channel mutant spread was only slightly greater than that of a nonmotile (Δ*motPS*) strain that remains a dense colony at the inoculation site (data not shown). As observed by phase-contrast microscopy, SC34 cells exhibited a "tumbly" phenotype relative to wild type. A tumble refers to the transient dispersal of the helical bundle of flagella during a random change of direction that occurs when smooth counterclockwise swimming is interrupted by a switch to clockwise motion (18). Restoration of the *ncbA* gene to the chromosome restored wild-type motility on soft agar and reduced the tumbliness, although not to a completely wild-type pattern. Transformation of either wild-type or SC34 with a multicopy plasmid encoding *ncbA* led to stronger motility and slightly greater tumbliness than observed in a control wild-type transformant;

the pSC-Ca plasmid did not enhance motility of either the wild-type or SC34 strains.

After 24 h of incubation, flanged outcroppings of more motile bacteria appeared at the edge of SC34 colonies (MYE soft agar plates; pH 10.5). Repeated transfer from that edge to soft agar plates yielded the stable up-motile SC34-M strain. SC34-M was just as tumbly as its SC34 progenitor strain but even more motile in the soft agar plate assay than wild-type-M (Table 1). The greater migration of SC34-M than wild-type-M on soft agar plates is probably an example of "pseudotaxis" (19), in which greater migration in soft agar is found in bacterial mutants with an increased clockwise flagellar rotation bias relative to their wild-type parent. This greater motility was retained, and the tumbliness of SC34-M was not entirely reversed by restoration of *ncbA* to the chromosome in SC34-MR (Table 1).

Increased tumbliness is associated with defects in chemotaxis, the motility-based behavior whereby bacteria respond to temporal gradients of attractants and repellants (20–22). Bacteria extend smooth runs toward an attractant by reducing their tumbling frequency and increase tumbling in response to repellants, thereby increasing the chance of moving in a new direction away from the repellant. The interesting possibility of a chemotaxis defect in *ncbA* mutants was assessed by using a capillary assay of pH 10.5-grown strains of up-motile wild-type-M, SC34-M, and SC34-MR that swim well enough for use of this assay. The low nutrient condition compromises pH homeostasis, so a pH of 8.5 was used instead of pH 10.5. The *ncbA* mutant SC34-M exhibited an inverse chemotaxis phenotype relative to the wild-type-M in these assays (top of Table 2). Although the wild-type-M exhibited positive chemotaxis (i.e., moved toward aspartate, proline and glucose), SC34-M

Table 3. Mutational loss of Na$_V$BP and MotPS affect pH homeostasis in alkaline-shifted cells

| | Cytoplasmic pH (pH$_{in}$) and $\Delta\Psi$ 10 min after a pH 8.5 → 10.5 shift | | | |
| | 100 mM added Na$^+$ | | 2.5 mM added Na$^+$ | |
Strain	pH$_{in}$	$\Delta\Psi$, mV	pH$_{in}$	$\Delta\Psi$, mV
Wild type	8.46*	−173	9.03	−161
SC34 ($\Delta ncbA$)	8.66	−178	9.43	−159
SC34-R ($\Delta ncbA$, ncbA restored)	8.48	−170	9.02	−158
Mot6 ($\Delta motPS$)	8.52	−169	9.03	−155
SC34/Mot6 ($\Delta ncbA$, $\Delta motPS$)	8.72	−177	9.51	−138

*The values are mean values from at least two independent experiments in which cells equilibrated at pH 8.5 were subjected to shift of pH$_o$ to 10.5. The standard deviations of the mean for pH$_{in}$ were ≤2% and for $\Delta\Psi$ were ≤5%.

exhibited negative chemotaxis. Upon *ncbA* restoration in SC34-MR, positive chemotaxis toward aspartate was restored, although the response was quantitatively reduced relative to that of wild-type-M. The *ncbA* mutant also exhibited an inverted response to high pH. Wild-type-M exhibited negative chemotaxis to nonnutrient buffer at pH 10.5 (middle of Table 2) but exhibited positive chemotaxis when malate was included in the capillary; there was no response to malate alone. SC34-M exhibited an opposite pattern to that of wild-type-M, moving toward pH 10.5 buffer in the absence of malate and away from pH 10.5 when malate was present. Finally, if loss of Na$_V$BP indeed accounts for the inverse chemotaxis behavior of SC34-M, then a channel inhibitor should elicit inverse chemotaxis by wild-type-M strain. As shown in the bottom of Table 2, the Na$_V$BP inhibitor Nifedipine (1) caused inversion of the chemotaxis response of wild-type-M to aspartate.

A pH Homeostasis Defect Results from Deletion of *ncbA* and Is Exacerbated in an *ncbA-motPS* Double Mutant. The pH homeostasis capacities of pH 8.5-equilibrated wild-type and SC34 cells were first compared upon a sudden alkaline shift to pH 10.5 in the presence of 50 mM sodium malate; malate is a nutrient that enters the cell with Na$^+$. Both strains had a postshift cytoplasmic pH of 8.2 under these conditions, as seen earlier for the wild type (14) (data not shown). In subsequent assays, pH 8.5-equilibrated cells of these strains were shifted to nonnutrient buffer at pH 10.5 containing 100 or 2.5 mM Na$^+$. The SC34-R strain (*ncbA* restored), the motility mutant Mot6, and the double *ncbA* and *motPS* mutant SC34/Mot6 were also tested. The wild type exhibited better pH homeostasis with 100 mM than with 2.5 mM Na$^+$ but even at the higher [Na$^+$], its cytoplasmic pH was near 8.5 (Table 3) vs. 8.2 when malate was present. In the presence of 100 mM Na$^+$, the channel mutant SC34 and the double mutant showed a marginal deficit in pH homeostasis relative to the wild-type and Mot6 strains (Table 3). With 2.5 mM Na$^+$ present, all of the strains exhibited greater alkalinization of the cytoplasm than with 100 mM Na$^+$, but there were strain-specific differences. The Mot6 and wild-type strains had the same postshift cytoplasmic pH of 9.03 (13), whereas the SC34 strain exhibited a pH homeostasis defect that was abolished upon restoration of chromosomal *ncbA* (Table 3). The double $\Delta ncbA \Delta motPS$ mutant exhibited even greater cytoplasmic alkalinization than SC34 and also exhibited a deficit in $\Delta\Psi$ generation. Higher $\Delta\Psi$ is generated by *B. pseudofirmus* OF4 as the pH$_o$ is raised from 7.5 to 10.5, and the pH homeostatic mechanism acidifies the cytoplasm (12). In the presence of 2.5 mM Na$^+$, which is suboptimal for pH

homeostasis, $\Delta\Psi$ generation after a shift to pH 10.5 was lower in all of the strains than in the presence of 100 mM Na$^+$, but the double mutant exhibited a significant deficit relative to the other strains (Table 3). The $\Delta ncbA \Delta motPS$ mutant also exhibited a growth defect at pH 10.5 but not pH 7.5 in complete medium. At pH 10.5, the growth yield of the double mutant on MYE was just over 50% that of wild-type or Mot6, and the doubling time of the mutant was ≈90 min vs. 70 min for wild-type, SC34, and Mot6.

Discussion

This study establishes Na$_V$BP as a voltage-gated Na$^+$ channel whose current amplitude is increased and activation range is hyperpolarized by high pH (Figs. 1 and 2) and shows that Na$_V$BP is important for motility, pH homeostasis, and chemotaxis in *B. pseudofirmus* OF4. The *ncbA* deletion mutant SC34 was poorly motile and regained a wild-type motility phenotype upon restoration of Na$_V$BP but not a Ca^{2+}-selective Na$_V$BP mutant (Table 1). The motility defect of SC34 was also well compensated in the SC34-M variant that arose after prolonged incubation on soft agar plates at pH 10.5, although the chemotaxis-related defects remained. This suggests that altered expression of another alkaliphile channel may substitute for the Na$_V$BP role in motility but not chemotaxis and may prevent full reversal of the inverse chemotaxis phenotype and the "pseudotactic" motility phenotype of SC34-M upon *ncbA* restoration (Tables 1 and 2).

The contribution of Na$_V$BP to pH homeostasis was evident during a sudden shift to high pH at low [Na$^+$], but Na$_V$BP does not have an exclusive role in Na$^+$ reentry. The minor growth phenotype of the *ncbA* mutant at pH 10.5 and the absence of a deficit in pH homeostasis after shifts to pH 10.5 in complete medium indicate that the Na$^+$ entering with solutes is the dominant source of Na$^+$ in complete medium. However, the significantly reduced growth of the double $\Delta ncbA \Delta motPS$ mutant in complete medium at pH 10.5 relative to wild-type, *ncbA*, and *motPS* mutants suggests that both Na$_V$BP and MotPS channels contribute to Na$^+$ reentry. In the absence of added nutrients and at suboptimal [Na$^+$], the $\Delta ncbA \Delta motPS$ mutant exhibited a more severe pH homeostasis deficit than the *ncbA* mutant (Table 3). The role of MotPS in pH homeostasis at high pH is apparently masked in the single *motPS* mutant by compensatory Na$_V$BP activity.

We hypothesize that the effects of Na$_V$BP on motility and pH homeostasis are mediated in part by changes in gene expression in response to a transiently higher cytoplasmic [Na$^+$] and lower $\Delta\Psi$ when the channel opens. The deficit in motility suggests that Na$_V$BP may be required for normal pH-dependent expression of genes for flagellar assembly and function. The Mrp antiporter system, the major Na$^+$/H$^+$ antiporter for cytoplasmic pH regulation in extreme alkaliphiles (10, 11), is constitutively expressed, but increased cytoplasmic [Na$^+$] and perturbation of $\Delta\Psi$ would probably increase this basal expression. Expression of *mrp* antiporter genes in *B. subtilis* is increased in *mrp* mutants that are deficient in Na$^+$ exclusion (23) and is also increased in response to alkaline shock (24).

The role of Na$_V$BP in alkaliphile chemotaxis is the only one of the three physiological roles of Na$_V$BP for which no alternative compensatory channel or transporter is evident. A specific channel that is required for bacterial chemotaxis has not been identified before, although there are many earlier indications of channel involvement in bacterial chemotaxis (25–30). Further studies of the details of the interaction of Na$_V$BP with the alkaliphile chemotaxis system may provide insights that illuminate roles of channels in bacterial chemotaxis in general, roles that may be more nuanced in nonextremophiles. The chemotaxis phenotype of the alkaliphile *ncbA* mutant is not secondary to a defect in pH homeostasis, because pH homeostasis was normal in malate-containing buffer, pH 10.5, whereas chemotaxis was

inverted. Inverse chemotaxis phenotypes can apparently result from a range of mutational perturbations of the signaling pathway or flagellar rotor switch (31–34). An appealing hypothesis is that Na_VBP colocalizes with the chemoreceptor array that usually is at the cell poles (35–38). Chemoreceptors might mediate signaling by high cytoplasmic and/or pH_o to shift the associated Na_VBP channels into the voltage range for activation and Na_VBP might have a reciprocal modulatory effect on chemosensory transduction.

The phenotypes of the *ncbA* mutant implicate Na_VBP as a positive element in activation of multiple cell functions at high pH. If so, Na_VBP activation in its natural setting must be responsive to some combination of a high pH_o and the secondary increases in cytoplasmic pH and $\Delta\Psi$ that occur in alkaliphile cells in the upper part of its pH range (12). In mammalian cells, we found that an increase in pH_o dramatically shifted the channel activation range toward more hyperpolarized potentials. Although the activation potential (≈ 100 mV at pH 9.0) is still not hyperpolarized enough to reach the bacterial transmembrane potential ($\Delta\Psi$, ≈ 160mV) at this pH (12), other triggers may open the channel in the bacterium. First, cytoplasmic pH rises in alkaliphilic bacteria in response to increases of pH_o above 9.5 (12), whereas the cytoplasmic pH of the mammalian cells in our experiments was controlled by pipette perfusion in the whole-cell configuration with Hepes-buffered at pH 7.4. The rise in cytoplasmic pH in alkaliphile cells when the pH_o exceeds 9.5 may provide an additional triggering stimulus for Na_VBP opening, allowing solute-independent Na^+ entry (10, 12). Second, the potential generated by the ΔpH (acid in) may directly, or indirectly by altering $\Delta\Psi$, modify the voltage sensing and opening of Na_VBP. Third, it is possible that $\Delta\Psi$ oscillates, or undergoes changes in response to stimuli, in a faster time frame than can be measured by the relatively slow measurements of $\Delta\Psi$ used in these bacteria. Fourth, the channel properties may be modulated by interaction with other proteins in its natural host, e.g., chemoreceptors. Our results suggest that the resulting channel activity supports several physiological functions at high pH, somehow facilitating proper chemotaxis responses while probably bolstering motility and pH homeostasis by a combination of direct effects on Na^+ entry and on expression of genes related to these physiological processes.

1. Ren, D., Navarro, B., Xu, H., Yue, L., Shi, Q. & Clapham, D. E. (2001) *Science* **294,** 2372–2375.
2. Yue, L., Navarro, B., Ren, D., Ramos, A. & Clapham, D. E. (2002) *J. Gen. Physiol.* **120,** 845–853.
3. Koishi, R., Xu, H., Ren, D., Navarro, B., Spiller, B. W., Shi, Q. & Clapham, D. E. (2004) *J. Biol. Chem.* **279,** 9532–9538.
4. Perriere, G. & Gouy, M. (1996) *Biochimie* **78,** 364–369.
5. Booth, I. R., Edwards, M. D. & Miller, S. (2003) *Biochemistry* **42,** 10045–10053.
6. Hirota, N., Kitada, M. & Imae, Y. (1981) *FEBS Lett.* **132,** 278–280.
7. Booth, I. R. (1985) *Microbiol. Rev.* **49,** 359–378.
8. Krulwich, T. A. (1995) *Mol. Microbiol.* **15,** 403–410.
9. Sugiyama, S. (1995) *Mol. Microbiol.* **15,** 592.
10. Krulwich, T. A., Ito, M. & Guffanti, A. A. (2001) *Biochim. Biophys. Acta* **1505,** 158–168.
11. Kitada, M., Kosono, S. & Kudo, T. (2000) *Extremophiles* **4,** 253–258.
12. Sturr, M. G., Guffanti, A. A. & Krulwich, T. A. (1994) *J. Bacteriol.* **176,** 3111–3116.
13. Ito, M., Hicks, D. B., Henkin, T. M., Guffanti, A. A., Powers, B., Zvi, L., Uematsu, K. & Krulwich, T. A. (June 22, 2004). *Mol. Microbiol.*, 10.1111/j.1365-2958.2004.04173x.
14. Ito, M., Guffanti, A. A., Zemsky, J., Ivey, D. M. & Krulwich, T. A. (1997) *J. Bacteriol.* **179,** 3851–3857.
15. Adler, J. (1973) *J. Gen. Microbiol.* **74,** 77–91.
16. Krulwich, T. A. & Guffanti, A. A. (1989) *J. Bioenerget. Biomemb.* **21,** 663–677.
17. Tadese, A. & Bean, B. P. (2002) *Neuron* **33,** 587–600.
18. MacNab, R. M. & Ornston, M. K. (1977) *J. Mol. Biol.* **112,** 1–30.
19. Wolfe, A. J. & Berg, H. C. (1989) *Proc. Natl. Acad. Sci. USA* **86,** 6073–6977.
20. Larsen, S. H., Reader, R. W., Kort, E. N., Tso, W.-W. & Adler, J. (1974) *Nature* **249,** 74–77.
21. Berg, H. C. (2003) *Annu. Rev. Biochem.* **72,** 19–54.
22. Aizawa, S.-I., Zhulin, I. B., Marquez-Magana, L. & Ordal, G. W. (2002) in *Bacillus subtilis and Its Closest Relatives: From Genes to Cells*, eds. Sonnenshein, A. L., Hoch, J. A. & Losick, R. (Am. Soc. Microbiol. Press, Washington, DC), pp. 437–452.
23. Ito, M., Guffanti, A. A., Wang, W. & Krulwich, T. A. (2000) *J. Bacteriol.* **182,** 5663–5670.
24. Weigert, T., Homuth, G., Versteeg, S. & Schumann, W. (2001) *Mol. Microbiol.* **41,** 59–71.
25. Ordal, G. W. (1977) *Nature* **270,** 66–67.
26. Gouldbourne, E. A., Jr. & Greenberg, E. P. (1983) *J. Bacteriol.* **153,** 916–920.
27. Omirbekova, N. G. Gabai, V. L., Sherman, M. Y., Vorobyeva, N. V. & Glagolev, A. N. (1985) *FEMS Microbiol. Lett.* **28,** 259–263.
28. Matsushita, T., Hirata, H. & Kusaka, I. (1988) *FEBS Lett.* **236,** 437–440.
29. Tisa, L. S., Olivera, B. M. & Adler, J. (1993) *J. Bacteriol.* **175,** 1235–1238.
30. Tisa, L. S. & Adler, J. (2000) *J. Bacteriol.* **182,** 4856–4861.
31. Togashi, R., Yamaguchi, S., Kihara, M., Aizawa, S.-I. & MacNab, R. M. (1997) *J. Bacteriol.* **179,** 2994–3003.
32. Muskavitch, M. A., Kort, E. N., Springer, M. S., Goy, M. F. & Adler, J. (1978) *Science* **201,** 63–65.
33. Khan, S., MacNab, R. M., DeFranco, A. L. & Koshland, D. E., Jr. (1978) *Proc. Natl. Acad. Sci. USA* **75,** 4150–4154.
34. Taylor, B. L. & Johnson, M. S. (1998) *FEBS Lett.* **425,** 377–381.
35. Maddock, J. R. & Shapiro, L. (1993) *Science* **259,** 1717–1723.
36. Harrison, D. M., Skidmore, H., Armitage, J. P. & Maddock, J. R. (1999) *Mol. Microbiol.* **31,** 885–892.
37. Kirby, J. R., Niewold, T. B., Maloy, S. & Ordal, G. W. (2000) *Mol. Microbiol.* **35,** 44–57.
38. Gestwicki, J. E., Lamanna, A. C., Harshey, R. M., McCarter, L. L., Kiessling, L. L. & Adler, J. (2000) *J. Bacteriol.* **182,** 6499–6502.

BIOCHEMISTRY